Probing and comparing electron doping and miss-site effects in Re-based double perovskites

2009 J. Phys.: Condens. Matter 21 216008

(http://iopscience.iop.org/0953-8984/21/21/216008)

J. Phys.: Condens. Matter **21** (2009) 216008 (9pp) doi:10.1088/0953-8984/21/21/216008

Probing and comparing electron doping and miss-site effects in Re-based double perovskites

J Blasco[1,5], J Sesé[2], J A Rodríguez-Velamazán[1,3], C Ritter[3] and J Herrero-Martín[4]

[1] Instituto de Ciencia de Materiales de Aragón, Departamento de Física de la Materia Condensada, CSIC-Universidad de Zaragoza, Pedro Cerbuna 12, E-50009 Zaragoza, Spain
[2] Instituto Universitario de Investigación en Nanociencia de Aragón, Departamento de Física de la Materia Condensada, Universidad de Zaragoza, E-50009 Zaragoza, Spain
[3] Institut Laue-Langevin, F-38042 Grenoble Cedex, France
[4] European Synchrotron Radiation Facility, Boîte Postale 220, F-38042 Grenoble Cedex, France

E-mail: jbc@unizar.es

Received 10 February 2009, in final form 5 April 2009
Published 1 May 2009
Online at stacks.iop.org/JPhysCM/21/216008

Abstract

We have studied the $Sr_{2-x}La_xFe_{1+x/2}Re_{1-x/2}O_6$ series in order to check how the increase in the number of Fe–O–Fe superexchange interactions affects the magnetic properties of this family of double perovskites. In these compounds the addition of La^{3+} can be compensated by an increase of the Fe^{3+} ratio leading to a non-electron-doped system. The unit cell of these samples expands on replacing Sr by La and the cationic ordering disappears for $x > 1$ samples. Spontaneous magnetization at 5 K is observed in a wide range of concentrations but the magnetization at 5 T decreases as the La content increases. This result may be explained in terms of a ferrimagnetic ground state of the double perovskite. The magnetic ordering temperature increases with increasing the La and Fe content in agreement with an increase in the number of Fe–O–Fe interactions. The comparison to the electron-doped samples suggests that this effect is not enough to explain on its own the stronger T_C-rise in $Sr_{2-x}La_xFeReO_6$ compounds.

(Some figures in this article are in colour only in the electronic version)

1. Introduction

Magnetic double perovskites, $Sr_2BB'O_6$ (B = Fe, Cr; B′ = Mo, Re, W), have attracted a great deal of current attention owing to the reports of tunnelling type magnetoresistance at room temperature and at low magnetic fields [1, 2]. In these compounds, the B and B′ atoms are arranged as rock-salt in the perovskite B site, giving rise to B and B′ sublattices [1–3]. Historically, the ferrimagnetism in these compounds was explained in terms of antiferromagnetic superexchange interactions between B and B′ sublattices [4]. However, recent band calculations for Sr_2FeMoO_6 [5] and Sr_2FeReO_6 [6] claim the existence of a strong hybridization of the transition metal t_{2g} states (Re 5d or Mo 4d and Fe 3d) via oxygen 2p states which would stabilize high temperature magnetism. Hence, a magnetic moment at the Mo (or Re) site is induced by the Fe magnetic moments through the above-mentioned hybridization and this is the reason to identify these double perovskites as ferromagnetic. The electronic structure would consist of localized majority spin Fe 3d electrons and itinerant minority Re/Mo d electrons giving rise to a half-metallic ground state.

Therefore, these materials are very promising for spintronic applications and there is current interest in increasing their Curie temperature in order to enhance the magnetoresistance at room temperature. In this way, the electron doping (hereafter denoted as e-doping) of FeMo-based compounds, achieved by substituting trivalent La for divalent Sr, seemed to be successful in increasing T_C [7–10]. However, this type of doping seems not to

[5] Author to whom any correspondence should be addressed.

work for other double perovskites such as $Sr_{2-x}La_xCrWO_6$ or $Sr_{2-x}La_xCrReO_6$ compounds. In the first case, a strong decrease of T_C is observed between $x = 0$ and 0.5 [11] whereas in the second case, the attempts to prepare single phases were unsuccessful due to the formation of competitive $Sr_{2-x}La_xCr_{1+x/2}Re_{1-x/2}O_6$ phases [12].

Furthermore, doped $Sr_{2-x}La_xFeMoO_6$ samples show both larger electrical resistance and a reduced saturation magnetization which is believed to be produced by antisite defects (ASD). ASD can occur if Fe and Mo (or Re) ions exchange their positions on the B and B′ sublattices. The amount of ASD is 50% when the cations are randomly distributed. Studies on Sr_2FeMoO_6 samples with different amounts of ASD have revealed a close connection between this type of defect and T_C in such a way that disordered samples show higher T_C [13]. This was ascribed to the strong superexchange Fe–O–Fe interactions whose number increases as ASD does.

One of the problems in the study of some double perovskites is related to the difficulty in obtaining samples free from these defects. Sr_2FeMoO_6 itself has never been prepared without ASD and the usual amount is around 15%. The doping increases this value [7, 14, 15] and therefore it is hard to differentiate between contributions arising from doping and from Fe–O–Fe superexchange interactions [14]. In this way, the study of related double perovskites could shed light on this subject. Sr_2FeReO_6 exhibits a negligible amount of ASD [16] and it is composed of Fe^{3+} and Re^{5+} cations [17]. We have found recently that $Sr_{2-x}La_xFeReO_6$ can be formed up to $x = 0.5$ and the replacement of Sr by La induces a strong T_C enhancement [18]. The doped samples show a relatively small amount of ASD although they are increasing with increasing doping ratio from <1% for $x = 0$ to 5.5% for $x = 0.5$. These results seem to support the efficiency of e-doping to increase T_C in Fe-based double perovskites but, in order to be sure, an evaluation of the Fe–O–Fe superexchange contributions is mandatory. The present study is devoted to this purpose. We have prepared and characterized $Sr_{2-x}La_xFe_{1+x/2}Re_{1-x/2}O_6$ compounds which correspond to a situation where the additional electrons injected by La^{3+} are compensated by the increase of the Fe^{3+} ratio (compared to Re^{5+}), leading to a non-e-doped system. The end-members of this series are the ferromagnetic Sr_2FeReO_6 on the one side and the $LaFeO_3$ on the other. This orthoferrite exhibits a strong antiferromagnetic Fe–O–Fe coupling with $T_N = 740$ K [19]. Along the series, the Fe occupation on the Re sites is increased as the Sr is replaced by La. This effect leads to an increase in the number of Fe–O–Fe interactions. Our purpose is to study how this increase affects both the crystal structure and the magnetic properties with the aim of performing comparisons with doped compounds. This comparison will allow us to gain insight into the effective role of both e-doping and Fe–O–Fe interactions in the magnetic properties of double perovskites.

2. Experimental details

We have synthesized $Sr_{2-x}La_xFe_{1+x/2}Re_{1-x/2}O_6$ ($x = 0$, 0.1, 0.3, 0.5, 0.7, 1, 1.5 and 1.8) compounds by solid state reaction in an inert atmosphere. Stoichiometric amounts of La_2O_3, $SrCO_3$, Fe_2O_3, ReO_3 and Re were mixed, ground and heated at 1100 °C for 2 h in a current flow of Ar. The ReO_3/Re ratio was adjusted to the theoretical Re valence (5+). The powder was pressed into pellets and sintered at 1200 °C for 3 h in the same atmosphere. The last step was repeated until the end of the chemical reaction was indicated by the absence of changes in the x-ray patterns.

The samples were characterized by x-ray powder (XRD) diffraction using a Rigaku D-Max system. We used a graphite monochromator to select the Cu Kα radiation. All of the samples were single-phase. Step-scanned patterns were measured between 16° and 130° (in steps of 0.03°) at room temperature. The x-ray system was working at 40 kV and 80 mA with a counting rate of 5 s/step. The neutron powder diffraction study has been performed at the Institut Laue Langevin (Grenoble, France). The high intensity D1B diffractometer with $\lambda \sim 2.52$ Å was used to perform temperature scans between 300 and 700 K. The crystal structures were refined by the Rietveld method using the Fullprof program package [20].

Magnetic measurements were carried out using a commercial Quantum Design superconducting quantum interference device (SQUID) magnetometer. High temperature measurements were performed in a cooling cycle 800–300 K using a disposable sample holder as reported elsewhere [21].

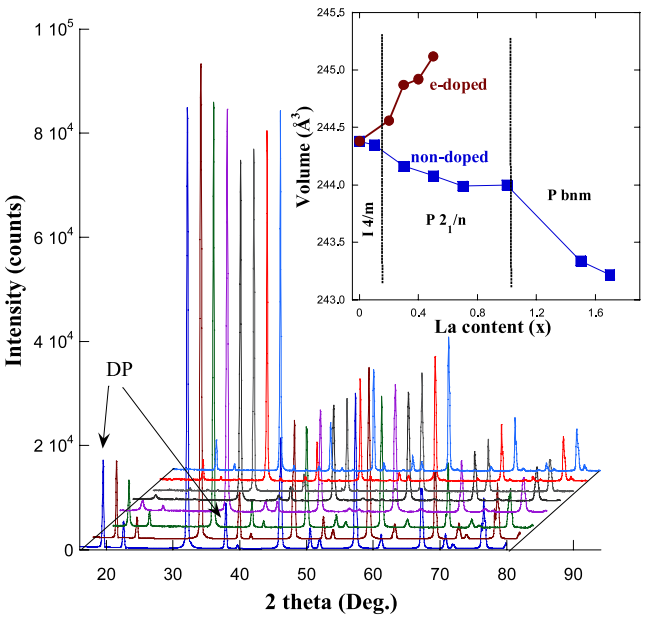

Figure 1. Detail of the x-ray patterns for $Sr_{2-x}La_xFe_{1+x/2}Re_{1-x/2}O_6$ samples (from bottom to top, $x = 0$, 0.1, 0.3, 0.5, 0.7, 1, 1.5 and 1.8). The patterns are shifted for the sake of clarity and arrows indicate the main peaks typical of cationic ordering. Inset: unit cell volume versus La content for $Sr_{2-x}La_xFeReO_6$ (e-doped) and $Sr_{2-x}La_xFe_{1+x/2}Re_{1-x/2}O_6$ (non-doped) compounds.

3. Results and discussion

$Sr_{2-x}La_xFe_{1+x/2}Re_{1-x/2}O_6$ ($0 \leqslant x \leqslant 1.8$) were obtained as black powders whose x-ray patterns are typical of a perovskite structure. Figure 1 shows a detail of these patterns for all

Table 1. Lattice parameters and reliability factors (defined as in [20]) obtained from the x-ray refinement of $Sr_{2-x}La_xFe_{1+x/2}Re_{1-x/2}O_6$ compounds at 300 K. Numbers in parentheses refer to standard deviations of the last significant digits.

Sample	$Sr_{1.9}La_{0.1}$	$Sr_{1.7}La_{0.3}$	$Sr_{1.5}La_{0.5}$	$Sr_{1.3}La_{0.7}$	SrLa	$Sr_{0.5}La_{1.5}$	$Sr_{0.2}La_{1.8}$
Space group	$I4/m$	$P2_1/n$	$P2_1/n$	$P2_1/n$	$P2_1/n$	$Pbnm$	$Pbnm$
a (Å)	5.5600(1)	5.5869(1)	5.5846(1)	5.5838(1)	5.5835(1)	5.5693(1)	5.5634(2)
b (Å)	—	5.5637(1)	5.5632(1)	5.5614(1)	5.5599(1)	5.5587(1)	5.5622(1)
c (Å)	7.9042(1)	7.8552(1)	7.8563(1)	7.8571(1)	7.8599(1)	7.8603(1)	7.8597
β (deg)	—	89.99(1)	90.01(1)	89.99(1)	90.01(1)	—	—
Volume (Å^3)	244.35(1)	244.16(1)	244.08(1)	243.99(1)	244.00(1)	243.34(1)	243.22(1)
R_{Bragg} (%)	2.9	4.4	3.0	3.3	4.6	4.6	3.5
R_{wp} (%)	9.1	8.1	7.2	7.2	8.9	9.1	9.0

Table 2. Refined fractional atomic coordinates, occupancies at Fe/Re sites (%Fe:%Re) and temperature factors at room temperature. Average bond lengths and bond angles for Fe and Re atoms. An average temperature factor was refined for all oxygen atoms. The atoms are placed in $I4/m$ as Sr at (4d), Fe at (2b), Re at (2a), O1 at (4e) and O2 at (8h): x y 0. For the $P2_1/n$, they are as Fe at (2c), Re at (2d), O and La/Sr at (4e). For $Pbnm$: La/Sr and O1 at (4c), O2 at (8d) and Fe/Re at (4b). Numbers in parentheses refers to standard deviations of the last significant digits.

Sample	$Sr_{1.9}La_{0.1}$	$Sr_{1.7}La_{0.3}$	$Sr_{1.5}La_{0.5}$	$Sr_{1.3}La_{0.7}$	SrLa	$Sr_{0.5}La_{1.5}$	$Sr_{0.2}La_{1.8}$
Sr/La:							
x	1/2	−0.0088(8)	−0.0050(11)	−0.0067(11)	0.0039(5)	0.9949(3)	0.9940(2)
y	0	0.0025(13)	0.0081(6)	0.0126(2)	0.0136(2)	0.0216(1)	0.0263(1)
z	1/4	0.7494(6)	0.7490(5)	0.7473(9)	0.7534(6)	1/4	1/4
B (Å^2)	0.78(2)	0.91(2)	0.83(2)	0.96(3)	0.70(3)	0.36(2)	0.39(1)
O1:							
x	0	0.278(3)	0.273(3)	0.259(3)	0.245(4)	0.057(2)	0.067(2)
y	0	0.271(3)	0.264(4)	0.242(3)	0.237(3)	0.491(1)	0.488(1)
z	0.247(1)	−0.021(3)	−0.022(3)	−0.008(3)	0.030(3)	1/4	1/4
O2:							
x	0.271(2)	0.238(3)	0.229(3)	0.215(3)	0.209(3)	0.722(2)	0.715(2)
y	0.227(2)	0.240(3)	0.239(3)	0.227(3)	0.218(3)	0.280(2)	0.279(2)
z	0	0.510(3)	0.490(3)	0.482(3)	0.464(2)	0.035(1)	0.038(1)
O3:							
x	—	0.037(4)	0.042(3)	0.051(3)	0.041(3)	—	—
y	—	0.519(3)	0.521(3)	0.515(2)	0.511(2)	—	—
z	—	0.252(3)	0.254(3)	0.249(3)	0.252(3)	—	—
B (Å^2)	0.89(12)	0.75(15)	0.78(12)	0.91(16)	0.73(13)	0.48(10)	0.59(10)
Fe: Occup.	100:0	95:5	93:7	91:9	78.5:21.5	87.5:12.5	95:5
B (Å^2)	0.29(4)	0.29(4)	0.29(4)	0.22(7)	0.40(8)	0.23(2)	0.24(2)
Re: Occup.	5:95	20:80	32:68	44:56	71.5:28.5	—	—
B (Å^2)	0.18(1)	0.29(2)	0.16(2)	0.17(4)	0.27(8)		
⟨Fe–O⟩ (Å)	1.989	1.998	2.016	2.017	2.019	1.997	2.004
⟨Re–O⟩ (Å)	1.959	1.962	1.945	1.947	1.964	—	—
⟨Fe–O–Re⟩ (deg)	172.6	168.3	167.6	167.9	163.0	160.1	157.8

samples. Superstructure peaks arising from the Fe/Re rock-salt ordering are relatively strong for Sr_2FeReO_6 and samples with a low content of La. Their intensity decreases as the La content increases but they are still noticeable in the pattern of the $SrLaFe_{1.5}Re_{0.5}O_6$ sample. The compounds richer in La ($x \geqslant 1.5$) do not show the superstructure peaks and the patterns agrees with a primitive perovskite, i.e. with a solid solution of Fe and Re atoms (or fully disordered specimens). Another property of these patterns is the selective broadening of the superstructure peaks, not observed for the rest of the peaks. Such a broadening increases as the La content does and it may be ascribed to the structural strain produced by the increase of Fe atoms occupying the Re sites that bring disorder on the Fe/Re rock-salt array.

The results of the structural refinement are summarized in tables 1 and 2. The crystal structure changes along the series. These changes are related to the value of the tolerance factor t defined in our case as

$$t = \frac{\frac{(2-x)r_{Sr}+xr_{La}}{2} + r_O}{\sqrt{2} \times (\frac{(1+x/2)r_{Fe}+(1-x/2)r_{Re}}{2} + r_O)}$$

where r_{Sr}, r_{La}, r_O, r_{Fe} and r_{Re} stand for the tabulated ionic radii of Sr^{2+} (12-fold coordination), La^{3+} (12-fold), O^{2-} (6-fold), Fe^{3+} (6-fold) and Re^{5+} (6-fold), respectively [22]. Ideal cubic perovskites appear for $t = 1$. For $t < 1$, the strain is relaxed by cooperative tilts and rotations of the oxygen octahedra (ReO_6 and FeO_6 in our case). The crystal structures formed in simple and double perovskites by different kinds of tilts were studied in the past by Glazer [23] and Woodward [24], respectively. Sr_2FeReO_6 with $t = 0.965$ shows a tetragonal cell in agreement with a tilt system $a^0a^0c^-$ [23, 24]. $LaFeO_3$ with $t = 0.895$ exhibits the tilt system $a^+b^-b^-$ with an orthorhombic

cell whose space group is *Pbnm* (standard setting *Pnma*). For double perovskites, the tilt system $a^+b^-b^-$ gives rise to a monoclinic cell [24] whose space group is $P2_1/n$, a subgroup of *Pbnm*. In the $Sr_{2-x}La_xFe_{1+x/2}Re_{1-x/2}O_6$ series, we observe tetragonal cells for $x \leqslant 0.1$ ($t \geqslant 0.962$) and monoclinic cells for $x \geqslant 0.3$ ($t \leqslant 0.954$). A similar sequence has also been observed in related Re-based double perovskites [25]. Samples without cationic ordering show the orthorhombic cell typical of $LaFeO_3$.

Overall, the unit cell volume in the $Sr_{2-x}La_xFe_{1+x/2}Re_{1-x/2}O_6$ compounds decreases as the x value increases. Upon increasing x and according to the tabulated ionic radii [21], we substitute the small La^{3+} for the large Sr^{2+} whereas the small Re^{5+} is replaced by the large Fe^{3+}. The first effect is preponderant and the volume decreases. It is worth comparing this trend to the behaviour shown by the $Sr_{2-x}La_xFeReO_6$ series [18] (hereafter also denoted as e-doped compounds). This comparison is performed in the inset of figure 1. The e-doped series exhibits an expansion of the crystal cell upon increasing the x value, opposite to the behaviour of the $Sr_{2-x}La_xFe_{1+x/2}Re_{1-x/2}O_6$ (non-doped) series although in the former compounds only Sr^{2+} is replaced. This result is in agreement with an effective electron injection into the FeRe sublattice for the e-doped series where the expansion of the FeRe sublattice overcomes the shrinking of the Sr(La) one.

In the $Sr_{2-x}La_xFe_{1+x/2}Re_{1-x/2}O_6$ series, the Sr(La) sublattice shrinks whereas the FeRe one is expanding upon increasing x. Accordingly, t decreases and the octahedron rotations rise. This leads to a decrease of the average Fe–O–Re bond angle as indicated in table 2. With increasing La content the Fe excess is placed onto 'Re sites'. Refinement of the occupation suggests that this mixing of Fe and Re on the Re sites leads only slowly to a mixing as well on the Fe sites. In this way, both sites show nearly identical Fe:Re occupation for $x \geqslant 1$. In the case of the $SrLaFe_{1.5}Re_{0.5}O_6$, a primitive orthorhombic perovskite structure can be used to refine its x-ray patterns with good reliability factors. We have, however, still chosen the double perovskite model for this $x = 1$ compound due to the presence of very weak and broad superstructure reflections in the patterns which cannot be accounted for by the primitive perovskite structure. Such superstructure peaks are absent in the patterns of the $x > 1$ samples.

Neutron patterns were also measured for selected samples from room temperature up to 700 K. These patterns revealed a strong magnetic contribution at room temperature, which decreases as temperature increases. Figure 2(a) shows the temperature dependence of the first magnetic peak in the tested samples. The magnetic scattering can be mostly noticed on the (011) and (013) reflections. The spins lie in the *ab* plane for all samples as in related doped samples [18]. The exact direction cannot be determined from powder diffraction due to the small orthorhombic distortion of $0.3 \leqslant x \leqslant 1$ samples. Figure 2(a) clearly shows that the magnetic contribution appears at higher temperatures as x is increased. The increase of the magnetic transition temperature will be confirmed later by means of magnetic measurements. Moreover, the integrated intensity

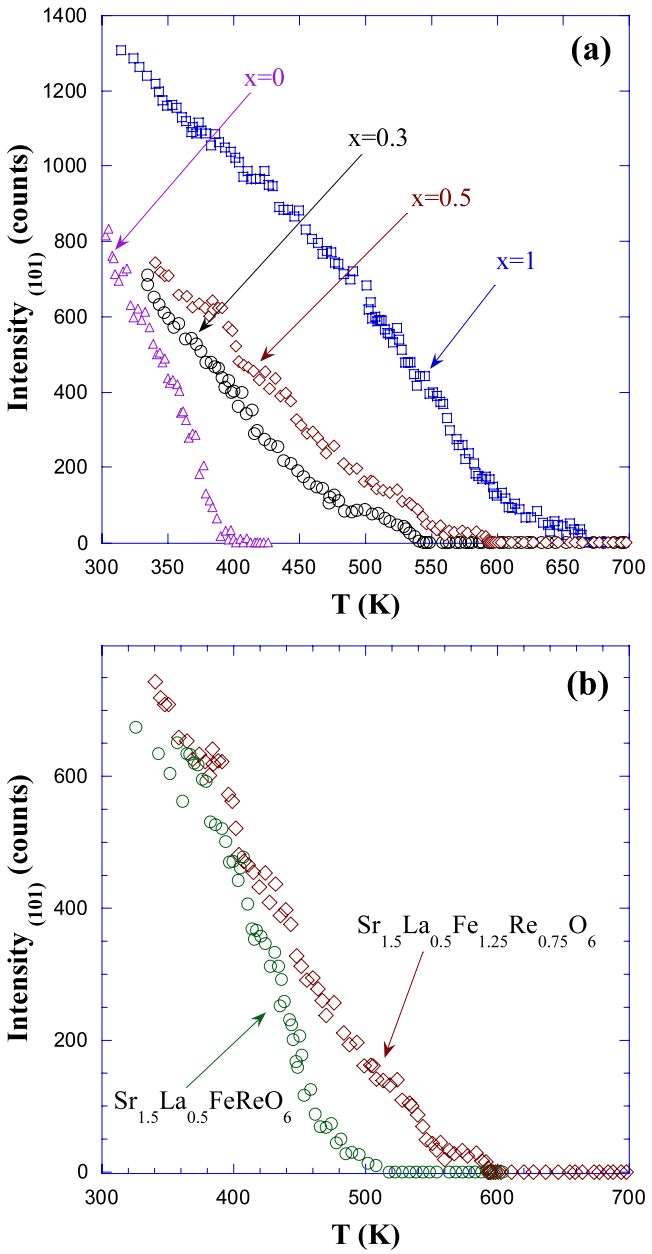

Figure 2. (a) Temperature evolution of the first magnetic peak intensity for $Sr_{2-x}La_xFe_{1+x/2}Re_{1-x/2}O_6$ samples ($x = 0$, 0.3, 0.5 and 1). (b) Magnetic peak intensity versus temperature for $Sr_{1.5}La_{0.5}Fe_{1.25}Re_{0.75}O_6$ and $Sr_{1.5}La_{0.5}FeReO_6$.

of the magnetic peaks is larger for La-rich samples. The form of the decay of the magnetic scattering with increasing temperature is striking. While Sr_2FeReO_6 shows an abrupt decay typical of a Brillouin function, the rapid decay is replaced by a more gradual diminution of the magnetic peak intensity for the rest of the samples. Figure 2(b) compares the temperature dependence of the intensity for the first magnetic peak between an e-doped sample and a non-doped sample with the same La content. The different behaviour is clearly noticeable.

The temperature dependence for the intensity of magnetic peaks in the non-doped samples resembles the findings in the disordered Sr_2FeMoO_6 compound [13]. In this case, the gradual intensity decay at high temperature was ascribed

to antiferromagnetic coupling between adjacent Fe^{3+} cations through Fe–O–Fe superexchange interactions. These interactions would naturally occur in $Sr_{2-x}La_xFe_{1+x/2}Re_{1-x/2}O_6$ samples due to the Fe excess occupying the Re sites. As the Fe population increases, these interactions become stronger and the magnetic contribution appears at higher temperature in the neutron patterns.

The magnetic properties were also studied by means of macroscopic measurements. Figure 3 shows the temperature dependence of the ac magnetic susceptibility for all samples. The curve of Sr_2FeReO_6 exhibits a strong anomaly at ∼390 K, indicating the ferromagnetic transition. A similar behaviour is observed for the $x = 0.1$ sample at higher temperature. On the other side of the series, the $x = 1.5$ and 1.8 samples show a magnetic transition at very high temperature (inset of figure 3). Here, the magnetic susceptibility below the transition is very small and it should be ascribed to the antiferromagnetic ordering of Fe atoms (partly replaced randomly by Re atoms) in a primitive perovskite cell. A higher Re content leads in this context to a less pure Fe sublattice and therefore to a decrease of Fe–O–Fe interactions and a decrease of T_N. For intermediate compositions, $0.3 \leqslant x \leqslant 1$, the susceptibility curves clearly show two anomalies. The high temperature transition agrees with the appearance of a magnetic contribution in the neutron patterns (compare figures 2 and 3) and hence, it indicates the true magnetic transition from a paramagnetic state to a spin ordering. Below the magnetic transition, a cusp is observed in the susceptibility curves. This cusp appears between 410 and 440 K for the four samples studied and there is no relationship between the cusp temperature and the sample composition as it remains almost constant for $0.3 \leqslant x \leqslant 0.7$. In order to clarify its origin we are going to focus our discussion on the $Sr_{1.5}La_{0.5}Fe_{1.25}Re_{0.75}O_6$ sample. Figure 4 shows the thermodiffractogram of this sample between 338 and 708 K. We observe the appearing of clear magnetic peaks at $T_N \sim$ 550 K as indicated in figure 2. This value is close to the inflection point of the susceptibility curve (figure 3). No additional new peaks were noticed below 400 K, discarding any new magnetic ordering. The only additional magnetic feature deducible from the neutron thermodiffractogram is the peculiar behaviour of the magnetic peak intensity as shown in figure 2(b). The inset of figure 4 shows the hysteresis loops collected for this sample at selected temperatures. At 600 K, the compound is paramagnetic, showing a typical linear dependence for the magnetization. At 500 K, spontaneous magnetization is observed in agreement with a ferrimagnetic ground state. Below the susceptibility cusp, the magnetization of the sample increases but the most noticeable difference between above and below the cusp temperature is a strong rise of the coercive field. Therefore, the magnetic anomaly at ∼415 K seems to be related to a change in the magnetic anisotropy of the compound. We suggest that a plausible explanation could be the formation of the magnetic ordering in two steps. The first transition at the highest temperature is due to the ordering of Fe moments by means of the strong Fe–O–Fe superexchange interaction. With decreasing temperature, Re cations become more and more polarized and, finally, participate in the magnetic ordering. This Re contribution

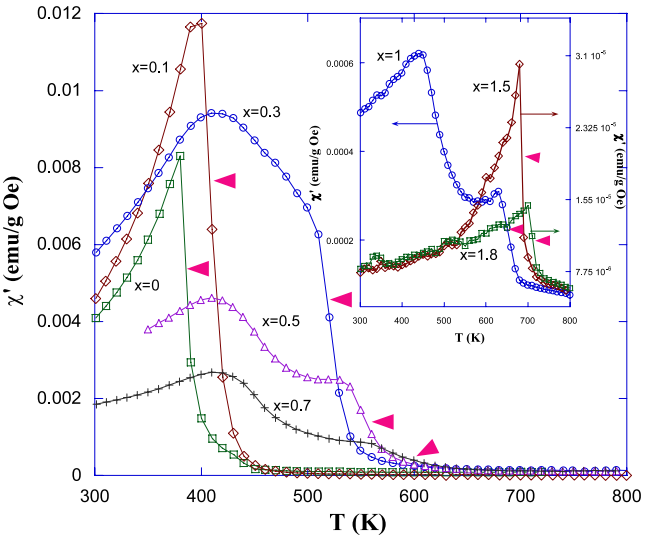

Figure 3. In-phase component of the ac magnetic susceptibility ($h_{ac} = 4$ Oe; $\upsilon = 10$ Hz) for $Sr_{2-x}La_xFe_{1+x/2}Re_{1-x/2}O_6$ samples ($x = 0$, 0.1, 0.3, 0.5, 0.7 and 1). Inset: comparison of the same curves for $x = 1$, 1.5 and 1.8. Ticks (triangles) mark the inflection point or magnetic transition.

should increase the magnetic anisotropy due to its intrinsic magnetic anisotropy, as will be discussed later. The magnetic coupling between near-neighbour Fe–Fe, Fe–Re or Re–Re is antiferromagnetic in agreement with superexchange rules and the resulting magnetic structure can be viewed as a ferrimagnet due to the atomic occupancies of both B sublattices ($x \leqslant 1$). Accordingly, the magnetic transition temperature increases with increasing La (and Fe) content, in agreement with the prominent role of the Fe–O–Fe superexchange interactions.

Figure 5(a) shows the magnetic isotherms at 5 K. All the samples with $x < 1.5$ exhibit hysteresis loops in agreement with a ferrimagnetic ground state. None of the samples achieves magnetic saturation at 5 T but all of them show a positive slope of the loop at high fields. This slope suggests a paramagnetic contribution in addition to the ferrimagnetism. The magnetization of the samples at 5 T decreases as x increases. This tendency may be explained on the basis of the changing atomic occupancies of the B sites of the double perovskite. As the Fe content increases on the Re site (see table 2), the difference in magnetic moment between both sublattices decreases. Disorder may also lead to the presence of paramagnetic regions, giving rise to inhomogeneous compounds from the magnetic point of view. The spontaneous magnetization for $x = 1.5$ at 5 K could be accounted for by a small canting of the antiferromagnetic structure although the presence of magnetic clusters cannot be discarded.

The hysteresis loops shown in figure 5(a) reveal that these compounds are behaving like very hard magnets at low temperature. The upper inset in figure 5(a) shows the values of coercive fields for $x \leqslant 1$ samples at 5 and 300 K. The coercive field for Sr_2FeReO_6 is ∼2560 Oe at 5 K and the coercivity rises with increasing La content up to concentrations of $x = 0.3$. Above this value, the coercivity decreases as x increases. The

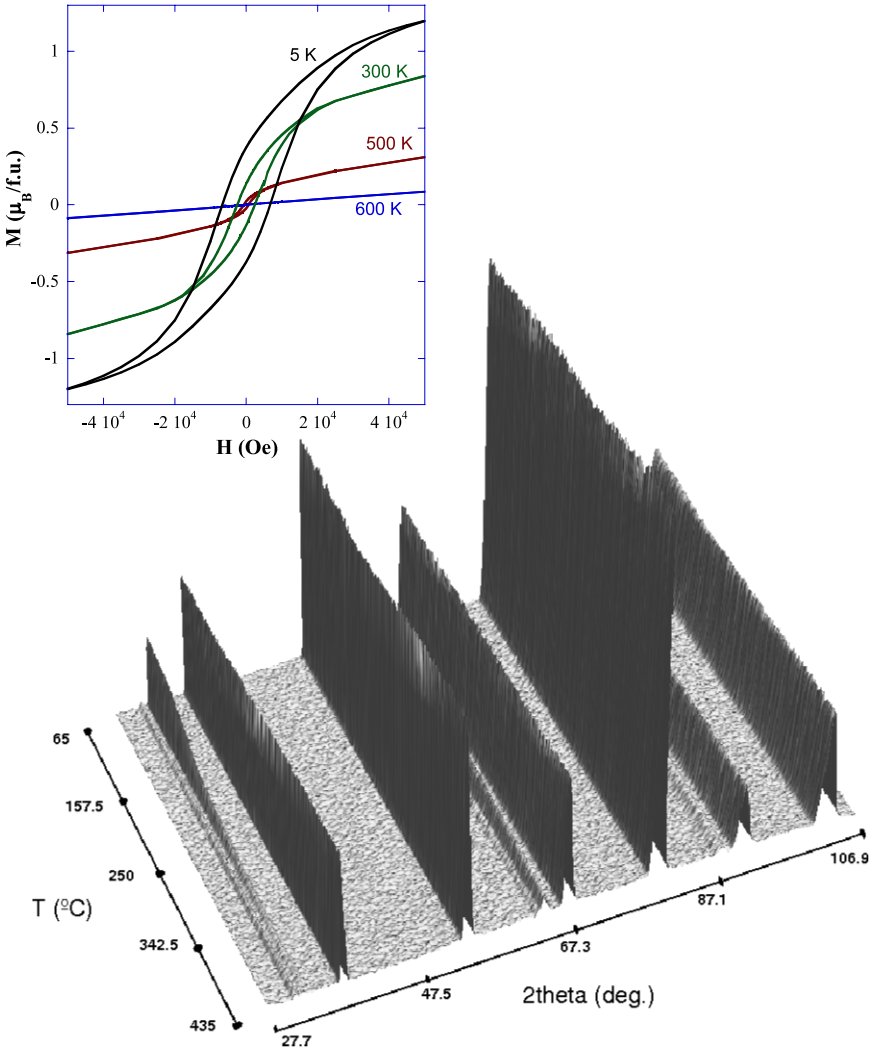

Figure 4. Neutron diffraction thermodiffractogram of $Sr_{1.5}La_{0.5}Fe_{1.25}Re_{0.75}O_6$. Inset: hysteresis loops for $Sr_{1.5}La_{0.5}Fe_{1.25}Re_{0.75}O_6$ at the temperatures indicated in the figure.

large value of the coercive field for these samples is the reason for the impossibility to achieve magnetic saturation at 5 T.

A ferrimagnetic component is also present at room temperature for $x \leqslant 1$, as can be seen in figure 5(b). The decrease upon warming of the magnetization at 5 T is as expected. However, the reduction of the value of the coercive field is surprisingly strong (upper inset in figure 5(a)). It decreases, for instance, between 5 and 300 K from ∼8500 Oe down to ∼1800 Oe in the case of $Sr_{1.7}La_{0.3}Fe_{1.15}Re_{0.85}O_6$ compound. Again at 300 K, the samples with $x = 0.3$–0.5 are the magnetically hardest although the maximum is shifted towards $x = 0.5$. These properties can be explained considering two sources of magnetic anisotropy. The first origin of anisotropy comes naturally from atomic disorder. There are two B sublattices with different atomic occupations so that a large variety of environments are expected for both atoms, Fe and Re. This effect is expected to increase as cationic ordering is decreasing due to the entry of Fe atoms into the Re sublattice and vice versa. Therefore, its maximum contribution is expected for samples around $x \sim 1$. On the other hand, a large coercive field has also been observed in Re-based double perovskites having no or low ASD. This property has been ascribed to a large intrinsic magnetic anisotropy caused by the interplay between spin–orbit coupling in Re^{5+} ions and crystal field effects [26]. This contribution is expected to decrease as the Re content decreases in the sample composition. Therefore, there are two sources of magnetic anisotropy and the balance between both contributions leads to the highest values of coercivity for compositions around $x \sim 0.3$–0.5.

Let us now turn to the discussion of the role of the number of available Fe–O–Fe paths in determining the magnetic transition temperature. It has become clear that an increase in the number of Fe–O–Fe paths (hereafter denoted as $N_{Fe-O-Fe}$) leads to an increase in the magnetic ordering temperature, in agreement with previous reports [13, 14, 27]. Remembering our original motivation for the study of the non-doped $Sr_{2-x}La_xFe_{1+x/2}Re_{1-x/2}O_6$ compounds the next step consists in the evaluation of this contribution in the e-doped compounds. With this aim, we have compared the evolution of T_C or T_N (ferromagnetic e-doped and ferrimagnetic non-doped samples) versus $N_{Fe-O-Fe}$. $N_{Fe-O-Fe}$ for each sample was calculated as indicated in the appendix. We have used

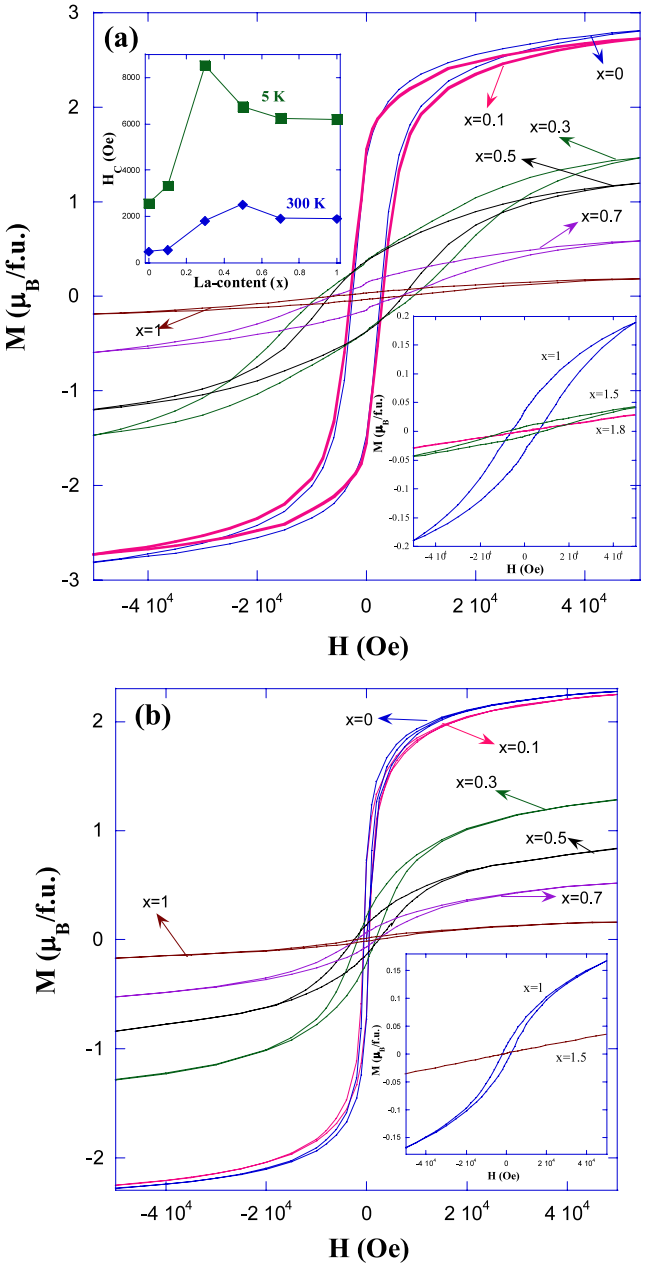

Figure 5. (a) Hysteresis loops for $Sr_{2-x}La_xFe_{1+x/2}Re_{1-x/2}O_6$ at 5 K and $x \leqslant 1$. Upper inset: coercive field versus composition for $Sr_{2-x}La_xFe_{1+x/2}Re_{1-x/2}O_6$ ($x \leqslant 1$). Lower inset: loops for $x = 1$, 1.5 and 1.8 samples. (b) Hysteresis loops for the same samples at 300 K. Inset: loops for $x = 1$ and 1.5 samples. The value of x is given for each curve in the figure.

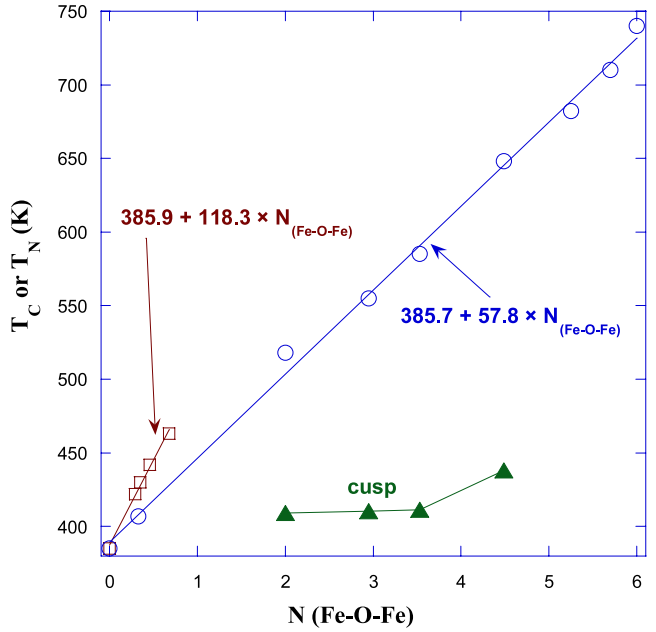

Figure 6. Temperature evolution of the magnetic temperature ordering versus the average number of Fe–O–Fe paths. Squares refer to $Sr_{2-x}La_xFeReO_6$ samples [18] whereas circles stand for $Sr_{2-x}La_xFe_{1+x/2}Re_{1-x/2}O_6$ compounds studied in the present survey. T_N of $LaFeO_3$ ($x = 2$) was taken from [19]. Linear fits and the best fit parameters are also included in the figure. Triangles denote the cusp temperature of magnetic susceptibility for non-doped samples.

occupancies from table 2 for non-doped compounds and data reported in [18] for e-doped samples. The results are collected in figure 6. In both series, the ordering temperature rises as the La content increases but, assuming a linear dependence, the slope is clearly different. In the case of e-doped compounds, the increase is very high with a slope of 118 $K/N_{Fe-O-Fe}$. This value is significantly higher than the one for non-doped compounds, ~58 $K/N_{Fe-O-Fe}$.

Electronic and structural effects overlap quite frequently and they must be tested carefully in order to obtain a reliable description about the influence of both effects. The unit cell volume follows an opposite trend for the two compared series. Usually, the strength of the magnetic interaction is directly related to the distance between the magnetic atoms but in perovskites it is also important how the atoms are linked. An important factor related to structural parameters is the bare electronic bandwidth W which has been approximated to the empirical formula $W \propto \cos w/(d_{M-O})^{3.5}$, where w is the tilt angle in the plane of the bond, $w = (\pi - \langle Fe–O–Re\rangle)/2$ in our case, and d_{M-O} is the M–O bond length (M = Fe or Re). Both structural parameters are easily calculated from the data of table 2 and a phenomenological relationship between T_C and W has been found in related double perovskites [28]. Tables 1 and 2 show that the volume reduction in the non-doped series is not related to a decrease of the M–O distance but to the smaller size of La^{3+} with respect to Sr^{2+}. This small misfit leads to the bending of the ⟨Fe–O–Re⟩ angle away from 180°. In fact, the average M–O bond length increases as the La content does, due to the increase of Fe^{3+} cations, bigger than Re^{5+}. Both effects, the increase of the M–O distance and the bending of the ⟨Fe–O–Re⟩ angle, should be detrimental to the superexchange interactions but in this series, T_N increases owing to the rise in $N_{Fe-O-Fe}$.

The doped series shows an expansion of the cell volume which is related to an increase in the Re–O bond length [18]. These compounds show a similar tilt for the ⟨Fe–O–Re⟩ bond angle. As both effects decrease W, the T_C increase should be ascribed to additional effects. One of these effects is also the increase of $N_{Fe-O-Fe}$ but the highest rise in T_C for the doped series directly points to the role of an effective increase of electron density within the d orbitals. Spectroscopic studies

indicated that additional electrons mainly go to the heavy metal states [29] in agreement with the increase of Re–O distances but our study reveals a relevant role for the counterpart cation because double perovskites having Fe show a T_C rise by e-doping [7–10] whereas such an effect is not reported for double perovskites without Fe [11, 30].

4. Conclusions

It is possible to prepare the whole $Sr_{2-x}La_xFe_{1+x/2}Re_{1-x/2}O_6$ series using ceramic procedures. Upon adding La, the unit cell volume decreases due to the smaller size of La^{3+}. This trend is opposite to the one found in $Sr_{2-x}La_xFeReO_6$ where an effective e-injection into the metal d bands is produced. In the former series, the simultaneous increase in La and Fe content in the samples is detrimental for the cationic ordering and the compounds became simple perovskites for $x > 1$. This substitution is also detrimental for the spontaneous magnetization value in agreement with a ferrimagnetic ground state for $Sr_{2-x}La_xFe_{1+x/2}Re_{1-x/2}O_6$ double perovskites. These compounds exhibit hysteresis loops with very large coercive fields. The highest value is achieved for $x \sim 0.3$–0.5 and two contributions are inferred for the magnetic anisotropy: the cationic disorder and the reported intrinsic magnetic anisotropy of Re^{5+} ions.

The magnetic ordering temperature increases with increasing the La content in the compound as also occurs in the $Sr_{2-x}La_xFeReO_6$ series. In the non-doped series, this increase is clearly ascribed to the rise in the number of Fe–O–Fe superexchange interactions. The number of Fe–O–Fe paths also increases in the e-doping series due to the increase of ASD but when comparing the effect of the number of Fe–O–Fe paths on the ordering temperature for both series, the T_C rise observed in e-doped compounds is significantly higher than the one expected from the sole Fe–O–Fe superexchange contribution. This confirms the effective role of the e-doping in the enhancement of T_C for the Fe-based double perovskites.

Acknowledgments

The authors acknowledge financial support from CICyT (project FIS08-03951) and DGA (CAMRADS). We thank ILL and SPINS for neutron beam time allocation. JS thanks MEC for the Ramón y Cajal contract.

Appendix

Double perovskites have two B sites (B and B′). Each atom in one of the sublattices (for instance B) is surrounded by six oxygens which are also linked to a B′ site. Hence, there are six B–O–B′ paths considering B as the central atom. In our compounds, both B and B′ are occupied by Fe and Re atoms in, normally, different proportions. Our task is to calculate the number of Fe–O–Fe paths from the refined occupancies (table 2). This is a problem of probability and combinations which can be better understood using an example. Take the $Sr_{1.7}La_{0.3}Fe_{1.15}Re_{0.85}O_6$ sample for instance. The B site is occupied by 95% Fe + 5% Re whereas B′ site is composed by 20% Fe′ + 80% Re′ (the apostrophe indicates atoms on the B′ site). The number of Fe atoms on the B site surrounded by six Re′ is given by $Re'(6) = ({}^6{}_6)0.8^6 = 0.262$, where $({}^6{}_6)$ is the binomial coefficient or choose function (1 in this case) and 0.8 is the occupancy (or ratio) of Re in each of the six possible B′ sites. Hence a 26.2% of Fe atoms in the B site is surrounded by six Re′ atoms. Following this procedure, the number of Fe surrounded by five Re′ and one Fe′ should be: $Re'(5) = ({}^6{}_5)0.8^5 \times 0.2 = 0.395$. Calculating all combinations, we obtain an average number of Fe–O–Re′ paths equal to 4.79 and Fe–O–Fe′ = 1.21 (total number of paths is six). This result is valid for atoms in the B site but there are also atoms in the B′ site with a different composition of neighbour cations. For an iron in the B′ site, the chance to be surrounded by six Fe (in B site) is $Fe(6) = ({}^6{}_6)0.95^6 = 0.735$ whereas the number of Fe′ surrounded by five Fe and one Re is $Fe(5) = ({}^6{}_5)0.95^5 \times 0.05 = 0.232$. Hence, the average Fe′–O–Fe is 5.7. In order to obtain the average number of Fe–O–Fe paths (no matter the B or B′ sublattice), we should calculate the weighted mean taking into account the Fe concentration on each site and the total amount of iron per formula unit. For the present example, it should be $N_{Fe-O-Fe} = (1.21 \times 0.95 + 5.7 \times 0.20)/1.15 = 1.99$. $N_{Fe-O-Fe}$ stands for the average Fe–O–Fe paths taking into account both sublattices.

References

[1] Kobayashi K I, Kimura T, Sawada H, Terakura K and Tokura Y 1998 *Nature* **395** 677
[2] Kim T H, Uehara M, Cheong S W and Lee S 1999 *Appl. Phys. Lett.* **74** 1737
[3] Blasco J, Ritter C, Morellón L, Algarabel P A, De Teresa J M, Serrate D, García J and Ibarra M R 2002 *Solid State Sci.* **4** 651
[4] Galasso F, Douglas F C and Kasper R 1966 *J. Chem. Phys.* **44** 1672
[5] Sarma D D, Mahadevan Pl, Sha-Dasgupta T, Ray T S and Kumar A 2000 *Phys. Rev. Lett.* **85** 2549
[6] Fang Z, Terakura K and Kanamori J 2001 *Phys. Rev.* B **63** 180407
[7] Navarro J, Frontera C, Balcells Ll, Martínez B and Fontcuberta J 2001 *Phys. Rev.* B **64** 092411
[8] Serrate D, De Teresa J M, Blasco J, Ibarra M R, Morellón L and Ritter C 2002 *Appl. Phys. Lett.* **80** 4573
[9] Rubí D, Frontera C, Nogués J and Fontcuberta J 2004 *J. Phys.: Condens. Matter* **16** 3173
[10] Hemery E K, Williams G V M and Trodahl H J 2006 *Phys. Rev.* B **74** 054423
[11] Philipp J B, Majewski P, Alff L, Erb A, Gross R, Graf T, Brandt M S, Simon J, Walther T, Mader W, Topwal D and Sarma D D 2003 *Phys. Rev.* B **68** 144431
[12] Blasco J, Michalik J M, García J, Subías G and De Teresa J M 2007 *Phys. Rev.* B **76** 144402
[13] Sánchez D, Alonso J A, García-Hernández M, Matínez-Lope M J and Martínez J L 2002 *Phys. Rev.* B **65** 104426
[14] Sánchez D, Alonso J A, García-Hernández M, Martínez-Lope M J, Casais M T and Martínez J L 2003 *J. Mater. Chem.* **13** 1771
[15] Ritter C, Blasco J, De Teresa J M, Serrate D, Morellón L, García J and Ibarra M R 2004 *Solid State Sci.* **6** 419
[16] Michalik J M, De Teresa J M, Blasco J, Algarabel P A, Ibarra M R, Kapusta Cz and Zeitler U 2007 *J. Phys.: Condens. Matter* **19** 506206
[17] Herrero-Martín J, Subías G, Blasco J, García J and Sánchez M C 2005 *J. Phys.: Condens. Matter* **17** 4963

[18] Blasco J, Rodríguez-Velamazán J A, Ritter C, Sesé J, Stankiewicz J and Herrero-Martín J 2009 *Phys. Rev.* B submitted
[19] Eibschütz M, Shtrikman S and Treves D 1967 *Phys. Rev.* B **156** 562
[20] Rodríguez-Carvajal J 1992 *Physica* B **192** 55 available at www.ill.eu/sites/fullprof/
[21] Sesé J, Bartolomé J and Rillo C 2007 *Rev. Sci. Instrum.* **78** 046101
[22] Shannon R D 1976 *Acta Crystallogr.* A **32** 751
[23] Glazer A M 1975 *Acta Crystallogr.* A **31** 756
[24] Woodward P M 1997 *Acta Crystallogr.* B **53** 32
[25] De Teresa J M, Serrate D, Blasco J, Ibarra M R and Morellon L 2004 *Phys. Rev.* B **69** 144401
[26] De Teresa J M, Serrate D, Blasco J, Ibarra M R and Morellón L 2005 *J. Magn. Magn. Mater.* **290/291** 1043
[27] Rubi D, Frontera C, Roig A, Nogués J, Muñoz J S and Fontcuberta J 2005 *J. Phys.: Condens. Matter* **17** 8037
[28] Ritter C, Ibarra M R, Morellón L, Blasco J, García J and De Teresa J M 2000 *J. Phys.: Condens. Matter* **12** 8295
[29] Navarro J, Fontcuberta J, Izquierdo M, Avila J and Asensio M C 2004 *Phys. Rev.* B **70** 054423
[30] Azad A K, Eriksson S G, Khan A, Svedlindh P and Irvine J T S 2008 *Phys. Rev.* B **77** 064418